N^6-methyladenosine-induced long non-coding RNA PVT1 regulates the miR-27b-3p/BLM axis to promote prostate cancer progression

BIN CHEN[1], CHANG LIU[2], HONG LONG[3], GUOHUI BAI[3], YUHANG ZHU[4] and HOUQIANG XU[1]

[1]Laboratory of Animal Genetics, Breeding and Reproduction in the Plateau Mountainous Region (Ministry of Education), College of Life Sciences, Guizhou University; [2]Guizhou University of Traditional Chinese Medicine, Guiyang, Guizhou 550025; [3]School of Stomatology, Zunyi Medical University; [4]Affiliated Hospital of Zunyi Medical University, Zunyi, Guizhou 563006, P.R. China

Received March 10, 2022; Accepted November 23, 2022

DOI: 10.3892/ijo.2022.5464

Abstract. Prostate cancer (PCa) is one of the most fundamental causes of cancer-related mortality and morbidity among males. However, the underlying mechanisms have not yet been fully clarified. The present study aimed to investigate the effects of plasmacytoma variant translocation 1 (PVT1) on the malignant behaviors of PCa cells and to explore the possible molecular mechanisms involved. The expression levels of PVT1 and microRNA (miRNA/miR)-27b-3p in PCa tissues and cell lines were measured using reverse-transcription-quantitative polymerase chain reaction. Methyltransferase 3 (METTL3)-mediated PVT1 N^6-methyladenosine (m^6A) modifications were detected using RNA immunoprecipitation (RIP) and RNA pull-down assays. Bioinformatics analysis was used to predict the interactions of miR-27b-3p with PVT1 and bloom syndrome protein (BLM), and these interactions were validated using RIP, dual-luciferase reporter and biotin pull-down assays. The functional importance of miR-27b-3p, PVT1 and BLM within PCa cells was assessed through the *in vitro* utilization of Cell Counting Kit-8, Transwell, wound healing and colony formation assays, and the *in vivo* use of a mouse xenograft model. The results revealed the high expression level of PVT1 in PCa tissues and cells, and epigenetic analyses revealed the upregulation of PVT1 expression following METTL3-mediated m^6A modification. PVT1 overexpression induced PCa cells to become more proliferative, migratory and invasive, whereas PVT1 knockdown led to the opposite phenotype. Furthermore, miR-27b-3p was found to target both PVT1 and BLM, and PVT1 functioned to sequester miR-27b-3p within cells, thereby indirectly promoting the BLM expression level. BLM overexpression reversed the adverse effects of PVT1 knockdown on the migratory, proliferative and invasive capabilities of PCa cells *in vitro* and *in vivo*. The overexpression of PVT1 contributed to the aggressive phenotype of PCa cells by regulating the miR-27b-3p/BLM axis. On the whole, the findings of the present study may provide novel potential targets for the treatment of PCa.

Correspondence to: Professor Houqiang Xu, Laboratory of Animal Genetics, Breeding and Reproduction in the Plateau Mountainous Region (Ministry of Education), College of Life Sciences, Guizhou University, 2708 South Section of Huaxi Avenue, Guiyang, Guizhou 550025, P.R. China
E-mail: xuhouqiangyx@163.com

Key words: prostate cancer, plasmacytoma variant translocation 1, N^6-methyladenosine modification, RNA methylation

Introduction

One of the most fundamental causes of cancer-related mortality and morbidity among males is prostate cancer (PCa) (1), with higher incidence rates observed in more developed countries (2,3). The etiology of PCa is complex and is dependent on a wide range of factors, such as age, genetics, lifestyle and environmental conditions (4,5). Although some new methods for the diagnosis and treatment of cancer have been developed, they are still in the experimental stage (6-8). The primary treatment for PCa is androgen deprivation therapy, which is associated with curative efficacy for those cases with early-stage disease (9,10). However, PCa is generally associated with poor outcomes attributable to poor screening efforts, low rates of successful curative treatment and high rates of therapeutic resistance. There is thus an urgent need to more clearly define the mechanistic basis for this disease, in order to identify novel biomarkers for improve patient outcomes.

The dynamic, reversible N^6-methyladenosine (m^6A) modification is the most commonly identified epigenetic alteration present in eukaryotic RNAs (11). Several enzymes regulate the m^6A modification (12), and the dysregulation of this process has been found to be associated with oncogenesis and malignant tumor behaviors owing to alterations in the expression levels of specific tumor suppressor genes or oncogenes within human cells (13,14). Long non-coding RNAs (lncRNAs) are transcripts of >200 nucleotides in length that have no coding potential (15). lncRNAs can regulate critical cellular processes, including autophagy, apoptosis, differentiation,

invasion and proliferation (16,17). Functionally, these lncRNAs can interact with RNAs and proteins to alter RNA splicing, RNA stability, microRNAs (miRNAs/miRs) activity, histone modifications, transcription, or translational activity (18). It has been demonstrated that lncRNAs are able to function as competing endogenous RNAs (ceRNAs), which can bind to specific miRNAs in a sequence-dependent manner, thereby sequestering them and indirectly regulating target gene expression (19,20). Furthermore, miRNAs can in turn regulate lncRNA expression (21). However, additional explorations are necessary for the meticulous understanding of the interaction among m^6A modification, lncRNAs, miRNAs and the progression of PCa.

The expression of lncRNA plasmacytoma variant translocation 1 (PVT1), located at 8q24.21 (22), is upregulated in PCa and multiple types of cancer (23,24). Despite such an upregulation, the specific mechanisms whereby PVT1 influences oncogenic activity have not yet been fully explored. Zhao *et al* (25) reported that STAT3 promoted PVT1 transcription by binding to specific sequences within its promoter region. Chen *et al* (26) found that the ALKBH5-mediated m^6A modification of PVT1 contributed to the tumorigenesis of osteosarcoma. However, to date, at least to the best of our knowledge, no study has determined whether there is a similar association between the m^6A modification status and PVT1 overexpression in PCa. Simiar to other lncRNAs, PVT1 is able to function as a ceRNA (27). In a previous study, PVT1 was shown to suppress miR-30d-5p, thereby enhancing gallbladder cancer cell proliferation and metastatic activity (28). Contrarily, another study reported the interaction of PVT1 with miR-619-5p within PCa cells in a manner conducive to tumor growth and gemcitabine resistance (29). Additional research, however, is essential to fully elucidate the miRNA-dependent mechanisms whereby PVT1 influences PCa cell behavior.

In the present study, it was hypothesized that PVT1 dysregulation may influence PCa onset and progression. Through a series of assays, it was ultimately found that PVT1 was capable of promoting PCa progression, in part by serving as a ceRNA for miR-27b-3p, thereby indirectly promoting bloom syndrome protein (BLM) upregulation. In addition, the methyltransferase 3 (METTL3)-mediated m^6A modification of PVT1 promoted its upregulation, influencing the PCa progression through the miR-27b-3p/BLM axis.

Materials and methods

Bioinformatics analysis. On the basis of the Oncomine (www.oncomine.org) and Gene Expression Omnibus (GEO; https://www.ncbi.nlm.nih.gov/geo/) databases, the differential expression of PVT1 between PCa tumors compared with healthy prostate tissues was analyzed. Based on The Cancer Genome Atlas (TCGA) database, the associations between PVT1 expression with sample type, Gleason scores, objective response rate and overall survival in PCa were assessed; moreover, the diagnostic and prognostic values of PVT1 were analyzed using receiver operating characteristic curve (ROC) analysis, which determined the area under curve (AUC).

The miRanda (https://tools4mirs.org/software/target_prediction/miranda/), miRwalk (http://mirwalk.umm.uni-heidelberg.de/), miRDB (https://mirdb.org/), RNA22 (https://cm.jefferson.edu/rna22/) and TargetScan (https://www.targetscan.org/vert_80/) databases were exploited to predict the target genes of miRNA. Potential miRNA binding partners for PVT1 were identified using the miRanda and the LncBase Predicted (ver. 2) online databases. The miRDB platform was applied to predict the target genes of miRNA.

Clinical samples. Tumor specimens and paired paracancerous tissues from patients with PCa were obtained from the Affiliated Hospital of Zunyi Medical University (Zunyi, China). A total of 12 samples were collected, including three paracancerous tissues, three benign prostate hyperplasia (BPH) tissues, three tissues with Gleason scores ≤7 and three tissues with Gleason scores >7. The clinicopathological data of the patients are presented in Table I. The study protocol was approved by the Ethics Committee of Affiliated Hospital of Zunyi Medical University [Compliance Medical Ethics Review (2021) no. 1-037]. Written informed consent was obtained from all participants prior to enrollment.

Cells and cell culture. LNCaP and PC3 human PCa cells and RWPE-2 cell lines were acquired from the American Type Culture Collection (ATCC) and cultured in a Dulbecco's modified Eagle's medium (DMEM) containing penicillin/streptomycin (Corning Inc.) and 10% fetal bovine serum (FBS; Gibco; Thermo Fisher Scientific, Inc.) in a 5% CO_2 humidified incubator at 37˚C.

Reverse transcription-quantitative polymerase chain reaction (RT-qPCR). TRIzol reagent was used for the extraction of total RNA using a reverse transcription kit (TransGen Biotech Co., Ltd.) according to the manufacturer's instructions, and it was subsequently used to prepare cRNA. qPCR was performed on a LightCycler System 2.0 (Roche Diagnostics GmbH) with the following thermocycling conditions: Initial pre-denaturation for 3 min at 94˚C, followed by 40 cycles of 95˚C with 10 sec, 60˚C for 10 sec and 76˚C for 20 sec; the evaluation of the solubility curve was performed at 95˚C for 5 sec and 65˚C for 1 min, which was followed by cooling at 42˚C for 30 sec. All experiments were performed in triplicate, and the relative gene expression was calculated using the $2^{-\Delta\Delta Cq}$ method (30). All the primers used for RT-qPCR are listed in Table SI.

Transfection assay. PVT1 or METTL3 knockdown was achieved using two PVT1 or METTL3-specific shRNAs (PVT1-sh1 and PVT1-sh2, METTL3-sh1 and METTL3-sh2), with a non-targeting shRNA (NC-sh) serving as a control (D03003, GenePharma Co., Ltd.). For PVT1 or BLM overexpression, the cDNA encoding PVT1 or BLM was reinforced via PCR and subcloned into the pcDNA3.1 vector (Invitrogen; Thermo Fisher Scientific, Inc.) to construct the pcDNA-PVT1 vector, with an empty vector serving as a negative control (pcDNA-NC). The miR-27b-3p mimic (5'-UUCACAGUGGCUAAGUUCUGC-3') and the appropriate negative control mimic (NC mimic, 5'-UUUGUACUACACAAAAGUACUG-3') were obtained from Guangzhou RiboBio Co., Ltd. The cells plated in six-well plates at a density of $1x10^6$ cells/well were transfected with the aforementioned shRNAs, plasmids, or mimics (PVT1-specific shRNAs and NC-sh, 50 nM; pcDNA-PVT1, pcDNA-BLM, and pcDNA-NC, 2 μg; miR-27b-3p mimic and

Table I. Baseline characteristics of the patients in the present study.

Tissue type	Case no.	Age, years	PSA	Volume (mm)	Gleason	Transfer
BPH	1	81	0.962	53x56x48	-	-
	2	83	1.232	61x54x60	-	-
	3	70	1.442	50x50x48	-	-
PCa	4	76	5.47	45x48x38	3+3	No
	5	70	2.23	35x46x29	3+3	No
	6	78	1.28	34x43x23	3+3	No
	7	71	68.48	35x35x37	4+5	Yes
	8	78	525.56	32x47x30	4+3	Yes
	9	75	118.1	51x78x47	4+5	Yes

NC mimic, 50 nM) using Lipofectamine 2000® (Invitrogen; Thermo Fisher Scientific, Inc.) according to the manufacturer's instructions. The cells were then used in subsequent experiments at 48-72 h post-transfection, and RT-qPCR was employed to verify the efficiency of transfection. All shRNA sequences are listed in Table SII.

Tumor xenograft assays. A total of 20 male 4-week-old BALB/c nude mice (weighing 18-22 g) were obtained from Zunyi Medical University and maintained under specific pathogen-free conditions (temperature, 24±2˚C; humidity, 50±15%) with free access to food and water in laminar airflow cabinets. Following 1 week for adaptation, a total of 20 mice were randomly divided into four groups to establish a mouse xenograft model. Briefly, the mice were subcutaneously implanted with control tumor cells or those that had been stably transfected with lenti-NC-sh or lenti-sh-PVT1 and pcDNA-BLM vector ($1x10^7$ cells) in 200 μl phosphate-buffered saline (PBS). After 7 days, tumor growth was controlled and tumor volume (mm^3) was measured as follows: Tumor volume=(length x $width^2$)/2. To ensure compliance with humane endpoints, the tumor diameter of the xenografts did not exceed 2 cm and the tumor volume was <4,400 mm^3. The mice were sacrificed 6 weeks later by cervical dislocation, and tumors were therefore harvested and weighed. The death of the mice was verified by signs of no breathing and no corneal reflex. The Guidelines for the Care and Use of Laboratory Animals were used to design all experiments, which received confirmation from the Ethics Committee of the Affiliated Hospital of Zunyi Medical University (ZMU21-2205-002).

All animal welfare considerations were taken, including efforts to minimize suffering and distress or special housing conditions. Animal health and behavior were monitored every day. According to the AVMA Guidelines on Euthanasia, if any ulceration or infection occurs in the tumor site, or the existed tumor interfere with eating or free movement, the animals should be euthanized.

Cell proliferation assay. Cell Counting Kit-8 (CCK-8) and colony formation assays were employed to assess cell proliferation. In CCK-8 assay, cells were seeded into 96-well plates (density, 2,000 cells/well) and incubated for 24, 48 and 72 h at 37˚C, and 10 μl CCK-8 reagent (Dojindo Laboratories, Inc.) were then added, followed by an additional incubation for 1 h at 37˚C. The absorbance was then measured at 450 nm.

Clonogenic assay. The PCa cells were cultured in DMEM supplemented with 10% FBS (1,000 cells/ml), and then seeded into 6-cm culture plates for 2-3 weeks. The culture medium was then changed and the cells were rinsed three times with PBS. Following fixation with 4% paraformaldehyde (PFA) for 15 min at room temperature, the cells were stained with Giemsa (Beyotime Institute of Biotechnology) for 20 min at room temperature, and all colonies consisting of >50 cells were counted under a microscope (Leica Microsystems GmbH) (31).

Cell migration and invasion assays. Wound healing assays were employed for measuring cell migration as previously described (32). Briefly, the cells were seeded in six-well plates at a confluency of 100%, and a 20 μl pipette tip was then used to generate a linear scratch wound in the cell surface. The cells were then further cultured for 48 h in serum-free medium. Wound closure was then imaged using an Olympus 1X71 camera system (Olympus Corporation) at 0 and 48 h post-wounding.

Transwell assays were used to assess cell invasion. Briefly, the cells were added to Transwell inserts (8-μm pore size, $5x10^4$ cells/well), and DMEM containing 20% FBS was added to the lower chamber. The cells were then incubated for 24 h at 37˚C, in which a cotton swab was utilized for the elimination of non-invasive cells, and the remaining cells were fixed with 4% PFA for 20 min at room temperature, stained with hematoxylin (Beyotime Institute of Biotechnology) for 15 min at room temperature, and counted under a light microscope (Olympus Corporation).

Western blot analysis. RIPA buffer (Beyotime Institute of Biotechnology) with protease inhibitor cocktail (Roche Diagnostics Inc.) was used for the extraction of proteins from cells. The protein concentration was determined using a BCA kit (Beyotime Institute of Biotechnology). Proteins were subsequently separated through 10% sodium dodecyl sulfate-polyacrylamide gel electrophoresis (SDS-PAGE), transferred onto polyvinylidene difluoride (PVDF) membranes (Millipore Sigma), and the blots were blocked with 5% non-fat milk in TBST prior to a 12-h incubation with antibodies

specific for rabbit cyclin D1 (1:1,000, cat. no. 55506), CDK6 (1:1,000, cat. no. 13331), CDK4 (1:1,000, cat. no. 12790), Bax (1:1,000, cat. no. 5023), Bcl-2 (1:1,000, cat. no. 4223), cleaved caspase-3 (1:1,000, cat. no. 9664), cleaved caspase-9 (1:1,000, cat. no. 7237), E-cadherin (1:1,000, cat. no. 3195), N-cadherin (1:1,000, cat. no. 13116), Vimentin (1:1,000, cat. no. 5741S), METTL3 (1:1,000, cat. no. 96391), BLM (1:1,500, cat. no. 2742), c-Myc (1:1,000, cat. no. 9402), or Slug (1:1,000, cat. no. 9585S) (all form Cell Signaling Technology, Inc.) for 12 h at 4˚C. Anti-mouse β-actin (1:5,000, cat. no. 81115-1-RR, ProteinTech Group, Inc.) served as a loading control, of which incubation conditions were as follows: 12 h at 4˚C. Subsequently, the membranes were incubated with appropriate species-specific secondary antibodies (1:5,000, cat. no. A0208, Beyotime Institute of Biotechnology) for 2 h at room temperature before the visualization of protein bands using an ECL Western Blotting Substrate kit (cat. no. ab65623, Abcam).

Immunohistochemical staining. Paraffin-embedded tissues sections were deparaffinized, exposed to antigen retrieval, treated for blocking endogenous peroxidase activities, blocked using goal serum (Gibco; Thermo Fisher Scientific, Inc.), and incubated with antibodies specific for BLM (1:200; cat. no. 15161-1-AP, ProteinTech Group, Inc.), proliferating cell nuclear antigen (PCNA; 1:200, cat. no. 10205-2-AP; ProteinTech Group, Inc.), cleaved caspase-9 (1:200; cat. no. 9509, Cell Signaling Technology, Inc.), or N-cadherin (1:400; cat. no. 13116; Cell Signaling Technology, Inc.) overnight at 4˚C, followed by 2 h-incubation with an appropriate secondary antibody (1:4,000; cat. no. ab205718; Abcam) at room temperature, and imaging using a phase-contrast microscope (cat. no. DMi1, Leica Microsystems GmbH).

Dual-luciferase reporter assay. Bioinformatics tools were employed to estimate the complementary sites of binding for miR-27b-3p within PVT1 and the BLM 3'-UTR. WT or mutated (MUT) versions of the predicted miR-27b-3p binding site were cloned into the pmirGLO vector (Promega Corporation) to prepare a reporter construct. The PC3 and LNCap cells were subsequently co-transfected with 2 μg of these reporter constructs and either 50 nM of miR-27b-3p mimics or corresponding controls using Lipofectamine 2000® (Invitrogen; Thermo Fisher Scientific, Inc.). Moreover, at 48 h post-transfection, using a dual-luciferase reporter assay system (Promega Corporation), the Firefly fluorescence was normalized to the *Renilla* fluorescence to quantify the luciferase activity.

RNA immunoprecipitation (RIP). The RIP assay was performed using a Thermo Fisher RIP kit (Thermo Fisher Scientific, Inc.) according to the manufacturer's instructions. Briefly, RIP lysis buffer was utilized to lyse the cells, followed by lysate incubation with human anti-AGO2 (1:1,000, cat. no. 2897, Cell Signaling Technology, Inc.), anti-BLM (1:1,500, cat. no. 2742, Cell Signaling Technology, Inc.), or control mouse anti-IgG (1:2,000, cat. no. 7076, Cell Signaling Technology, Inc.) antibodies. RNA was then accumulated and assessed using RT-qPCR.

RNA pull-down assay. RNA pull-down assay was performed using synthesized PVT1 as a probe to detect miR-27b-3p and BLM by RT-qPCR. First, the DNA fragment with the whole PVT1 sequence was amplified by PCR using a T7-containing primer. The amplified products were then cloned into pRCR8 (Invitrogen; Thermo Fisher Scientific, Inc.). The biotin-labeled PVT1 was transcribed with the Biotin RNA Labeling Mix *In Vitro* (Roche Diagnostics) and T7 RNA polymerase (Roche Diagnostics). Subsequently, the samples were treated with RNase-free DNase I (Roche Diagnostics) and recycled using the QIA quick Nucleotide Removal kit (Qiagen Inc.). They were then purified using the RNeasy Mini kit (Qiagen Inc.). The PC3 and LNCap cells were transfected with pcDNA-PVT1 and pcDNA-NC prior to gathering for a 10-min incubation with specific cell lysates at room temperature. The cell lysates were mixed with biotin-labeled PVT1 (Wuhan Boster Biological Technology, Ltd.,) and then incubated for 1 h at 4˚C. Subsequently, streptavidin agarose beads (Invitrogen; Thermo Fisher Scientific, Inc.) were added into each binding reaction according to the manufacturer's protocol and the mixture was incubated for 1 h at 25˚C. After washing with the wash buffer, biotin-coupled RNA complex was pulled down by centrifugation at 3,000 x g for 5 min at 4˚C. Elution buffers (50 μl) were used to elute the complex. The eluate was collected, precipitated RNA was extracted using TRIzol® reagent (MilliporeSigma) and enriched miR-27b-3p and BLM were assessed using RT-qPCR.

Methylated RNA immunoprecipitation. Total RNA extracted from the PCa cells was immunoprecipitated using anti-m^{6}A (cat. no. ab151230, Abcam) and a Magna methylated RNA immunoprecipitation (MeRIP) m^{6}A kit (cat. no. 17-10499, MilliporeSigma) based on the provided instructions, following the chemical fragmentation of this RNA to ~100 nucleotides in length. M^{6}A-containing RNA enrichment was then assessed using RT-qPCR.

RNA stability analysis. To block new RNA synthesis, the polymerase II inhibitor, α-amanitin (100 nM, MilliporeSigma) was added to the culture medium for treating the transfected cells. At the designated time points (0, 2 and 4 h), the cells were collected and lysed to detect the RNA levels of PVT1 using RT-qPCR analysis.

RNA-fluorescence in situ hybridization (FISH) and subcellular fractionation. The subcellular localization of PVT1 was identified using the FISH technique. In line with the Ribo™ lncRNA FISH Probe Mix (Red) (Guangzhou RiboBio Co., Ltd.), the specific methods used were as follows: A slide was placed into a 24-well culture plate. The PC3 and LNCap cells were taken and seeded at 6x10^4 cells/well, reaching ~80% cell confluency. The slides were then removed and fixed with 1 ml 4% PFA. After being treated with protease K, glycine and ethyl phthalide reagent, the cells were joined with 250 μl prehybridization solution and incubated at 42˚C for 1 h. The pre-hybridization solution was removed and the 21-nt FISH probes (Guangzhou RiboBio Co., Ltd., were then added Cy3-aaaGTGAGTAGTCGGACGGAGGA) at 37˚C overnight. The cells were hybridized overnight at 42˚C. For immunofluorescence assay, the fixed cells were incubated

with the anti-Cy3 antibody (cat. no. ab52060, Abcam) in blocking buffer (1X PBS, 0.1% Triton, and 2 mg/ml bovine serum albumin) for 30 min PBS plus with Tween-20 (PBST) for 5 min each and incubated with the secondary antibody in blocking buffer for a further 30 min at the room temperature, followed by DAPI staining (cat. no. ab104139, Abcam) diluted with PBST. The cells were then observed and photographed under a fluorescence microscope (Olympus Corporation).

Cellular fractionation was performed as follows: Briefly, the cells were washed with ice-cold PBS, collected, spun down and re-suspended in ice-cold buffer I (10 mM Hepes, pH 8.0, 1.5 mM MgCl2, 10 mM KCl, 1 mM DTT) supplemented with protease inhibitor cocktail, followed by incubation for 15 min on ice to allow the cells to swell. Igepal-CA630 (MilliporeSigma) was then added at a final concentration of 1% (use 10% stock solution) followed by vortexing for 10 sec. Nuclei were collected by centrifuging 2~3 min at maximum speed 21,100 x g). The resultant supernatant was cytosolic fraction. Nuclei were then lysed in ice cold buffer II (20 mM Hepes, pH 8.0, 1.5 mM MgCl2, 25% (v/v) glycerol, 420 mM NaCl, 0.2 mM EDTA, 1 mM DTT) supplemented with protease inhibitor cocktail followed by vigorous rotation at 4˚C for 30 min and centrifugation for 15 min at 12,000 x g at 4˚C. The resultant supernatant was nuclear fraction. Both cytosolic and nuclear RNAs were extracted by Phenol-Chloroform-Isoamyl Alcohol mixture (cat. no. 77618, MilliporeSigma) followed by RT-qPCR analysis.

Cycloheximide (CHX) half-life assay. At 48 h post-transfection, 20 μg/ml CHX (MilliporeSigma) were added to the cell medium. At the designated time points (0, 2, 4 and 8 h), the cells were collected and lysed to detect the protein levels of BLM using western blot analysis.

Statistical analysis. SPSS18.0 (IBM, Inc.) and GraphPad Prism 7.0 (GraphPad Software Inc.) software were used to analyze the data. The analyses were repeated in triplicate. Survival outcomes were compared using Kaplan-Meier plots and the log-rank test. Pearson's correlation analysis was performed to analyze the expression of PVT1 and its potential target miRNAs. Quantitative data are expressed as the mean ± standard deviation (SD) and analyzed using a Student's t-test or one-way analysis of variance followed by Tukey's post hoc test using GraphPad Prism software. A two-sided P-value <0.05 was considered to indicate a statistically significant difference.

Results

The upregulation of PVT1 expression is related to poor survival outcomes of patients with PCa. Initially, the Oncomine and GEO databases (33-42) were used to evaluate PVT1 expression, and it was revealed that the PVT1 expression level was significantly upregulated in PCa tumors compared with healthy prostate tissues (Fig. 1A and B). In TCGA database, the PVT1 expression level was significantly related to the sample type and a higher Gleason score (Fig. 1 C). Considering the association between patient clinicopathological characteristics and the PVT1 expression level in patients with PCa, ROC curves suggested that PVT1 was accompanied by a high sensitivity when it was employed for the diagnosis of PCa (AUC, 0.903; Fig. 1D). Kaplan-Meier curves also suggested that a higher PVT1 expression level was related to more unfavorable survival outcomes of patients with PCa (Fig. 1E). In time-dependent ROC curve analyses, the AUC values corresponding to the 1-, 3- and 5-year survival rates were 0.990, 0.769 and 0.769, respectively (Fig. 1F). These findings thus indicated that PVT1 may be a prognostic biomarker for PCa.

METTL3-mediated m^{6}A modification promotes the upregulation of PVT1 expression. The potential functional role of PVT1 in PCa was assessed by analyzing its expression level in PCa tissue. The PVT1 expression level was markedly upregulated in PCa tumors compared with paired paracancerous tissues or BPH samples (Fig. 2A). Similarly, the PVT1 expression level was upregulated in the LNCap and PC3 PCa cell lines compared with the control RWPE-2 cells (Fig. 2B).

Epigenetic alterations are critical regulators of the processes governing PCa progression (43,44). In the present study, RIP assay was thus conducted to explore the association between the m^{6}A modification status and PVT1 upregulation using anti-METTL3 antibody, which is specific for the most prominent m^{6}A-modifying enzyme. METTL3 precipitation resulted in a noticeable PVT1 enrichment compared with control IgG precipitation in the tested PCa cell lines (Fig. 2C), whereas this effect was reversed following METTL3 knockdown, in which PVT1 enrichment was attenuated compared with control IgG (Fig. 2D), suggesting a potential role of METTL3 as a regulator of PVT1 expression level. To further confirm this potential regulatory association, a lentivirus encoding a METTL3-specific shRNA (METTL3-sh) was used to knockdown this enzyme in LNCap and PC3 cells. When α-amanitin was used to treat these two cell lines in order to disrupt the synthesis of RNA, METTL3 knockdown was found to significantly reduce the PVT1 half-life (Fig. 2E). METTL3 knockdown was successfully confirmed using qPCR and western blot analysis, and when PVT1 the expression level was assessed in these cells, it was found to be downregulated and positively associated with the METTL3 expression level (Fig. 2F), confirming the existence of interactions between PVT1 and METTL3. Overall, these results demonstrated that METTL3-mediated m^{6}A modifications may be associated with the upregulation and stabilization of PVT1 in PCa cells.

PVT1 overexpression enhances in vitro PCa cell proliferation, apoptotic resistance, invasion and migration. In order to explore the mechanisms through which PVT1 can regulate PCa cell functionality, lentiviral vectors were used to induce its overexpression in PC3 and LNCap cells, and RT-qPCR was employed to confirm the transfection efficiency (Fig. 3A). The overexpression of this lncRNA was noted to be associated with significant increases in PCA cell proliferation in CCK-8 and colony formation assays (Fig. 3B and C). In Transwell and wound healing assays, PVT1 overexpression was further found to enhance the PCa cell migratory and invasive capabilities (Fig. 3D and E). When cell cycle- and apoptosis-associated proteins were evaluated in these cells using western blot analysis, the levels of G1/S-phase checkpoint proteins (CDK4/6 and cyclin D1) were elevated following PVT1 overexpression, as was consistent with the level of pro-survival oncogenic proteins (Bcl-2), while the levels of pro-apoptotic

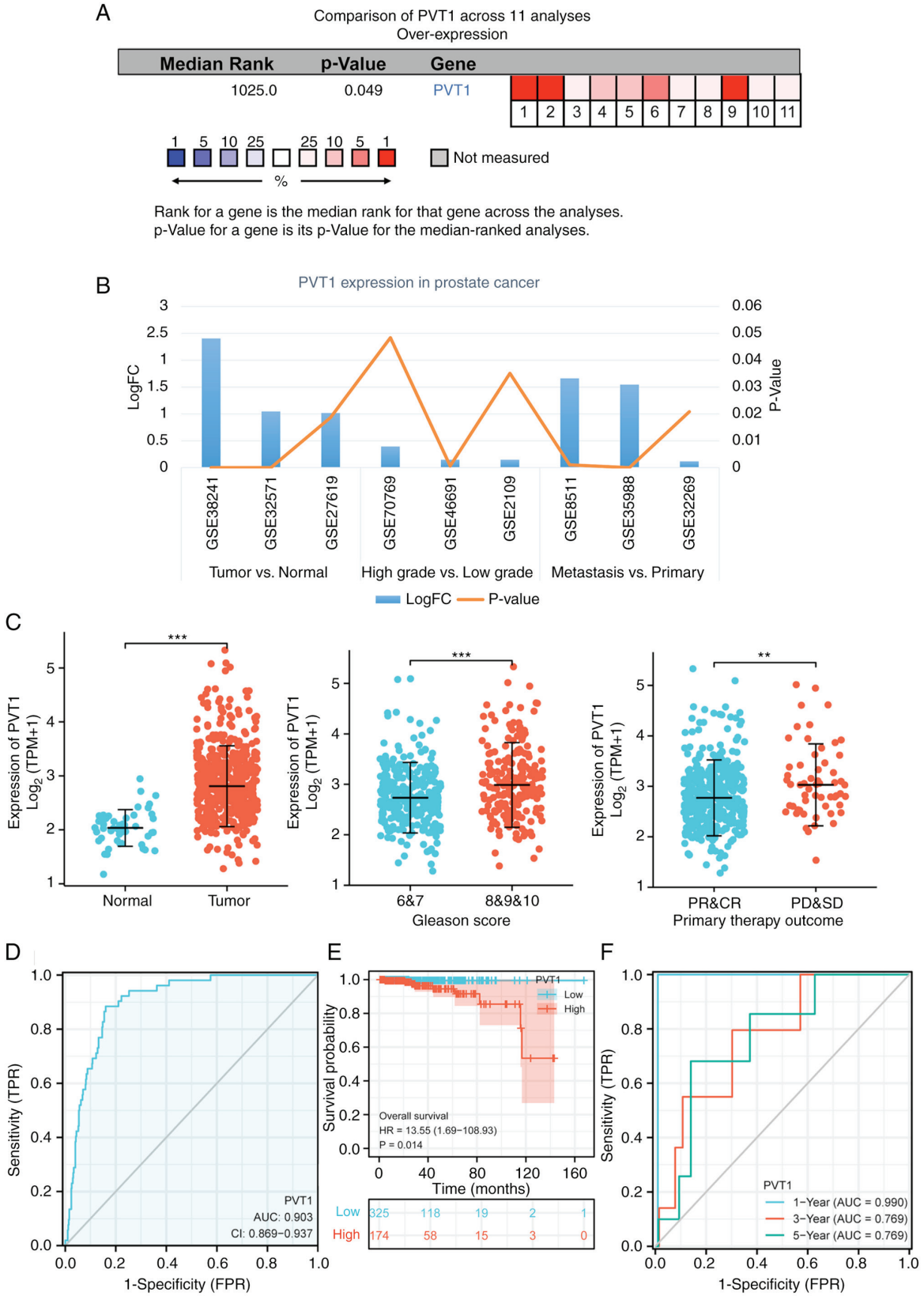

Figure 1. Analysis of the PVT1 expression level in PCa tissues and cells. (A) PVT1 expression level in PCa and normal tissues was detected using the Oncomine database. These datasets, in Arabic numerical order, were on prostate carcinoma vs. normal (33), prostate carcinoma vs. normal (34), prostate carcinoma vs. normal (35), prostate carcinoma vs. normal (36), prostate carcinoma vs. normal (37), prostate carcinoma vs. normal (38), benign prostatic hyperplasia stroma vs. normal (39), prostate carcinoma epithelia vs. normal (39), prostate carcinoma vs. normal (40), prostate carcinoma vs. normal (41), prostate carcinoma vs. normal (42). (B) The PVT1 expression level was compared between tumors and control tissues, and it was dependent on the sample type or histological grade. (C) PVT1 expression level in PCa and paired para-cancerous tissue samples from TCGA-PRAD database. (D) ROC curves corresponding to the PVT1 expression level in TCGA cohort. (E) Kaplan-Meier curves exploring the association between PVT1 expression level and overall survival of patients with PCa. (F) Time-dependent ROC curve-based analyses of the 1-, 3- and 5-year survival rates. **P<0.01 and ***P<0.001. PVT1, plasmacytoma variant translocation 1; PCa, prostate cancer; TCGA, The Cancer Genome Atlas; PRAD, prostate adenocarcinoma; CR, complete response; PR, partial response; SD, stable disease; PD, progressive disease; AUC, area under the curve; HR, hazard ratio.

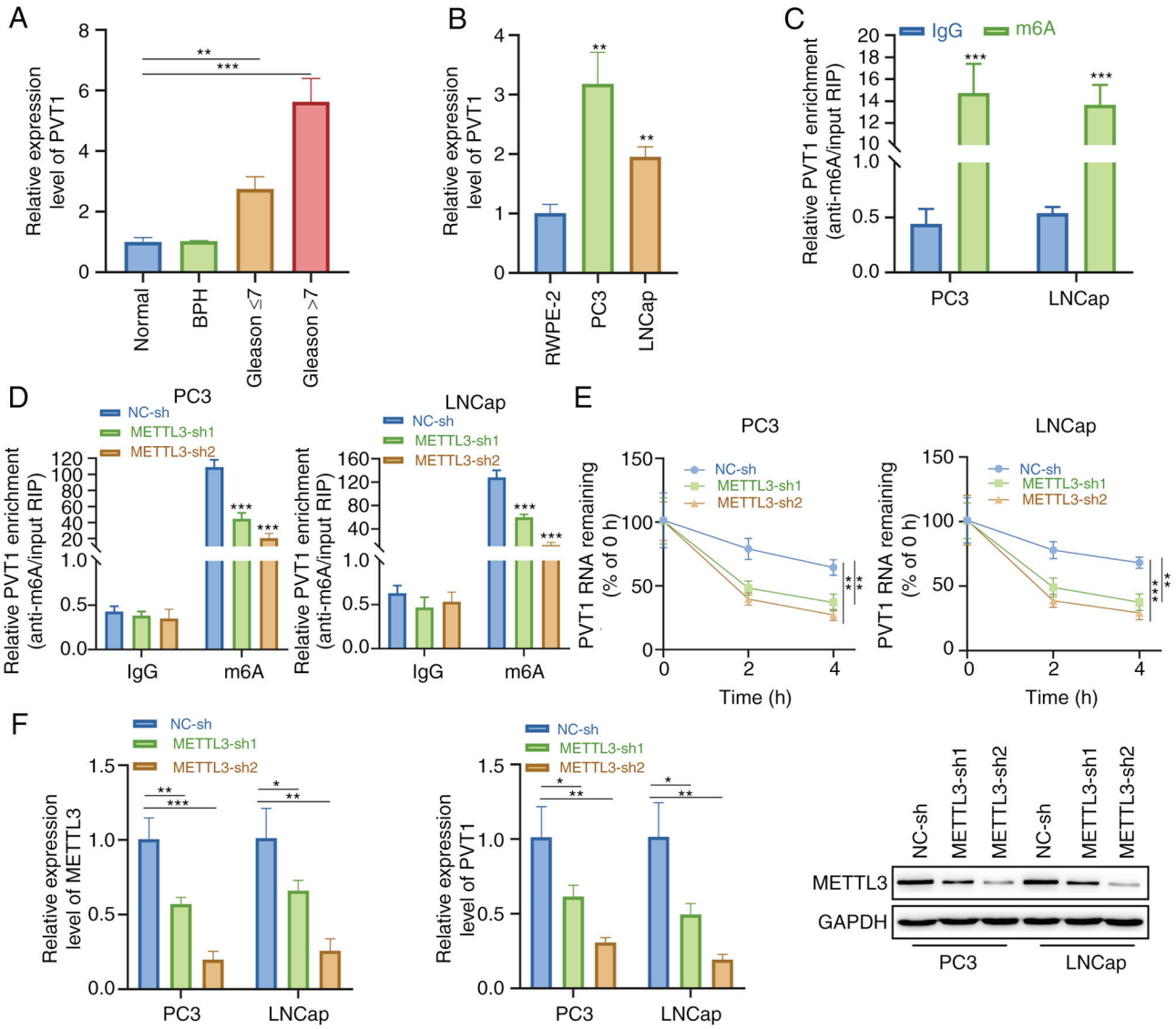

Figure 2. METTL3-mediated m^{6}A modification promotes PVT1 upregulation. (A) PVT1 upregulation was observed in PCa tissues compared with healthy or BPH tissues as determined using RT-qPCR. (B) PVT1 expression level in RWPE-2, PC3 and LNCap cells was measured using RT-qPCR. (C) Anti-m^{6}A antibody was used to conduct RIP assay. (D) Lentiviruses expressing shRNAs specific for METTL3 or corresponding negative control constructs were used to transduce PC3 and LNCap cells, and PVT1 expression level was then assessed following MeRIP-qPCR analysis conducted with anti-m6A. (E) α-amanitin (50 mM) was used to treat the PCa cells, in which METTL3 had or had not been knocked down, and RT-qPCR was used to assess PVT1 stability over time compared with baseline. (F) RT-qPCR and western blot analysis were respectively employed for detecting the expression levels of PVT1 and METTL3 in PC3 and LNCap cells, in which METTL3 had been knocked down. Data were from triplicate measurement and are presented as the mean ± SD. *P<0.05, **P<0.01 and ***P<0.001. m^{6}A, METTL3, methyltransferase 3; N^6-methyladenosine; PCa, prostate cancer; RT-qPCR, reverse transcription-quantitative polymerase chain reaction.

proteins (cleaved caspase-3/9 and Bax) were downregulated in these same cells (Fig. 3F). The overexpression of this lncRNA also inhibited the E-cadherin expression level, and increased the protein levels of Slug, Vimentin and N-cadherin in these PCa cells, which is consistent with the induction of epithelial-mesenchymal transition (EMT) (Fig. 3G). These data underscore the potential oncogenic role of PVT1 as a regulator of PCa cell malignancy *in vitro*.

Knockdown of PVT1 inhibits in vitro PCa cell proliferation, migration and invasion, whereas it induces cell death. Subsequently, shRNA constructs specific for PVT1 (PVT1-sh1and PVT1-sh2) or corresponding control constructs (NC-sh) were introduced into LNCap and PC3 cells, and PVT1 knockdown was confirmed using RT-qPCR (Fig. 4A). PVT1 knockdown suppressed the proliferation of these cells in both colony formation and CCK-8 assays (Fig. 4B and C). Moreover, PVT1 knockdown suppressed the invasive and migratory capabilities of the PCa cell lines in Transwell and wound healing assays (Fig. 4D and E). Consistently, the silencing of PVT1 also led to a marked decrease in the protein levels of CDK4/6, cyclin D1 and Bcl-2 together with concomitant increases in the levels of apoptosis-related proteins, such as cleaved caspase-3/9 and Bax (Fig. 4F). The silencing of PVT1 further enhanced the E-cadherin expression level, while it markedly suppressed the expression levels of Slug, Vimentin and N-cadherin compared with the control group (Fig. 4G). These results indicated that the knockdown of PVT1 decreased PCa cell malignancy.

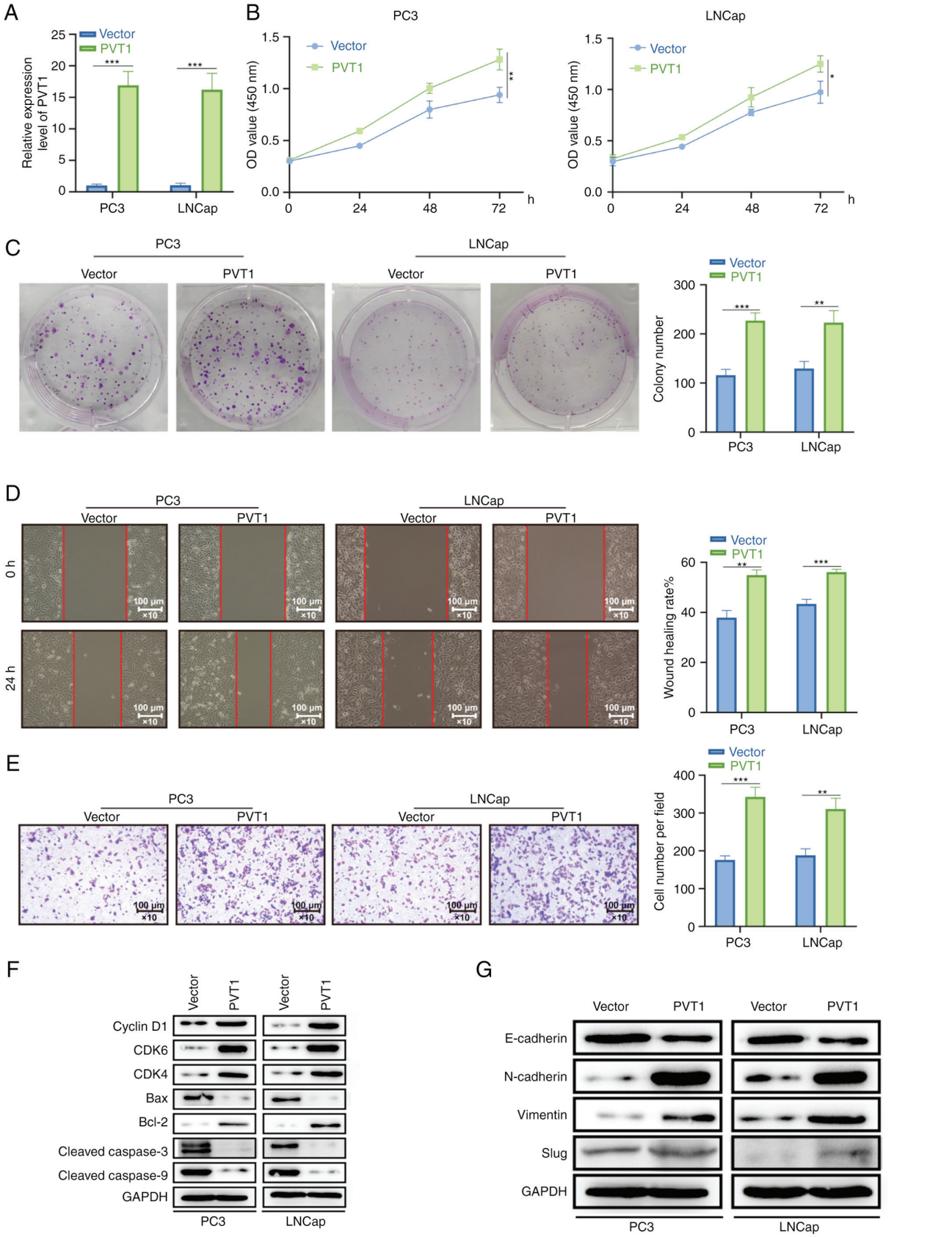

Figure 3. Effects of PVT1 overexpression on PCa cell behavior *in vitro*. (A) PVT1 upregulation in PC3 and LNCap cells treated with appropriate vectors was confirmed using reverse transcription-quantitative polymerase chain reaction. (B) PVT1 overexpression significantly enhanced the proliferative activity as evidenced using CCK-8 assay. (C) PVT1 overexpression enhanced colony formation activity of LNCap and PC3 cells compared with empty vector transfection. (D and E) PVT1 overexpression enhanced the migratory and invasive capabilities of LNCap and PC3 cells as evidenced using wound health and Transwell assays (magnification, x100; scale bars, 100 μm). (F) Western blot analysis was employed to evaluate cell cycle and apoptosis-related protein levels in the indicated PCa cells. (G) The expression levels of E-cadherin, N-cadherin, Vimentin and Slug were measured in the indicated PCa cells following PVT1 overexpression. Data were from triplicate measurement and are presented as the mean ± SD. *P<0.05, **P<0.01 and ***P<0.001. PVT1, plasmacytoma variant translocation 1; PCa, prostate cancer.

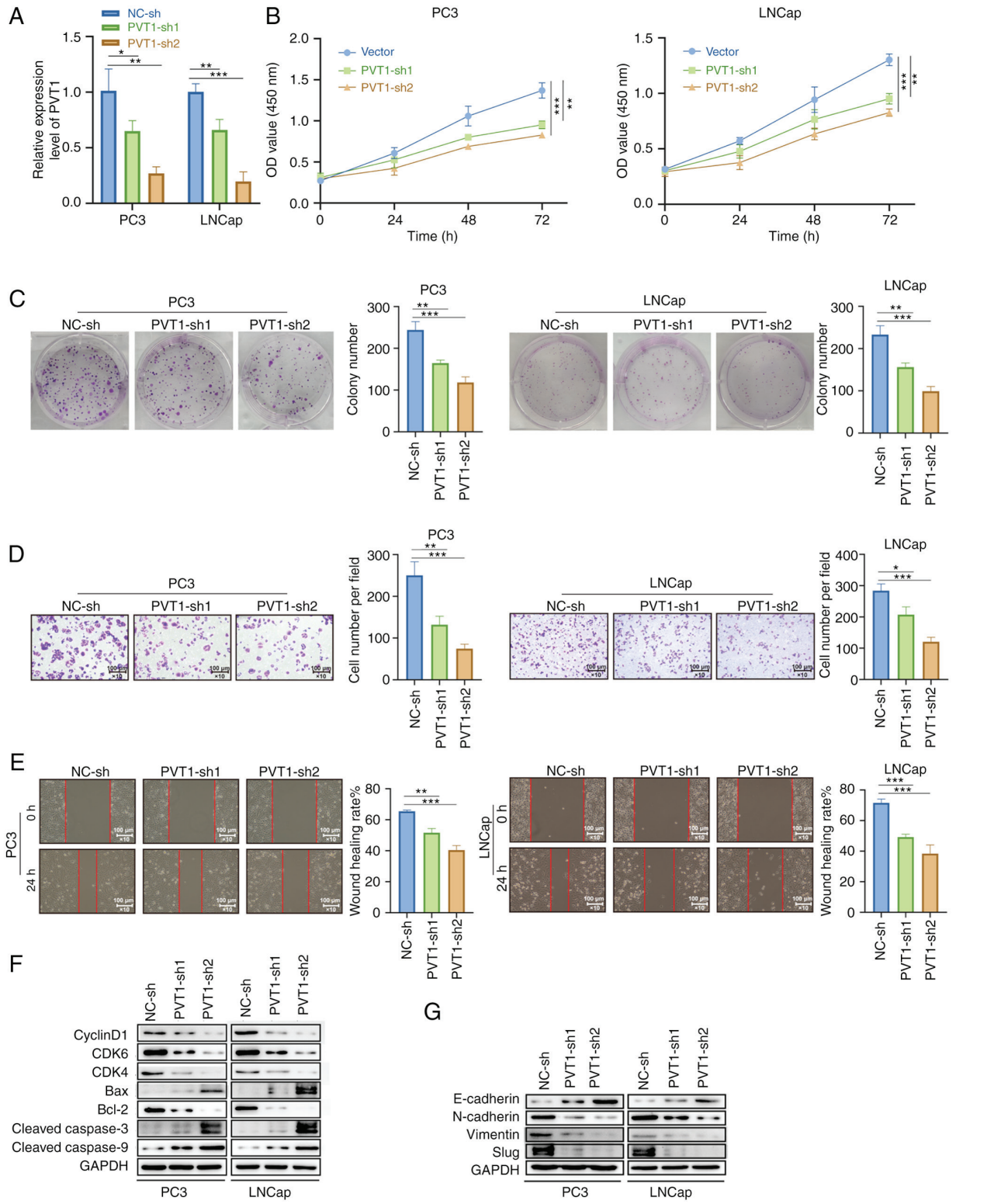

Figure 4. PVT1 knockdown alters the *in vitro* biological behavior of PCa cells. (A) Two siRNA constructs were employed to knockdown the PVT1 expression level in LNCap and PC3 cells. (B) The silencing of PVT1 significantly impaired PCa cell proliferation as shown by CCK-8 assay compared with NC-sh transfection. (C) The colony formation activity of LNCap and PC3 cells was reduced following PVT1 knockdown compared with NC-sh transfection. (D and E) The silencing of PVT1 inhibited the migratory and invasive capabilities of LNCap and PC3 cells as shown by wound healing and Transwell assays (magnification, x100; scale bars, 100 μm). (F) Cell cycle- and apoptosis-related protein levels were assessed in PCa cells following PVT1 knockdown. (G) The expression levels of E-cadherin, N-cadherin, vimentin and Slug were measured in the indicated PCa cells following PVT1 knockdown. Data were from triplicate measurement and are presented as the mean ± SD. *P<0.05, **P<0.01 and ***P<0.001. PVT1, plasmacytoma variant translocation 1; PCa, prostate cancer.

PVT1 functions as a ceRNA to sequester miR-27b-3p within PCa cells. When functioning as ceRNAs, lncRNAs are able to sequester miRNAs and thus indirectly promote the upregulation of their target mRNAs. In the present study, PVT1 was found to be primarily localized in the cytoplasm, rather than in the nucleus in RNA-FISH and

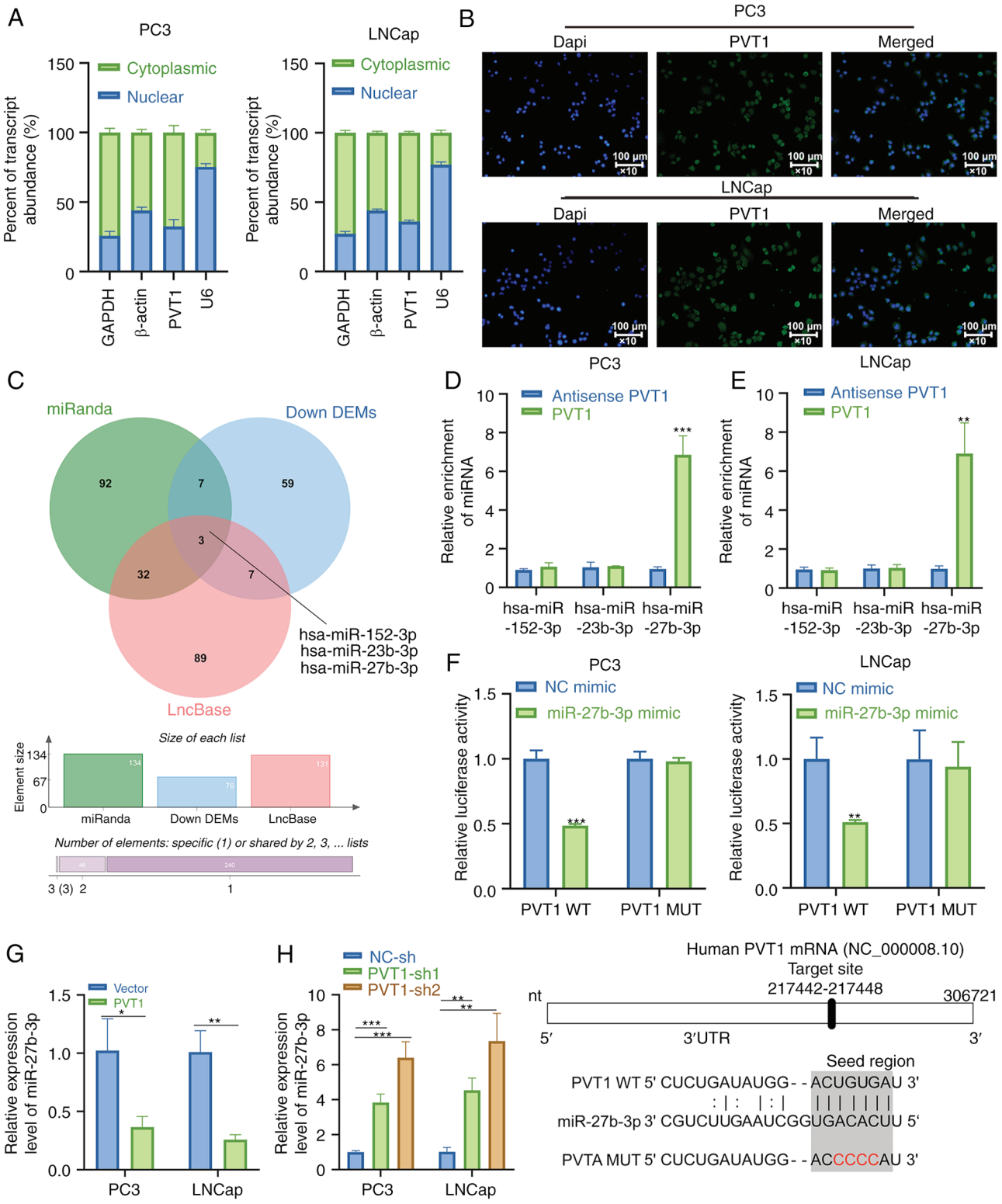

Figure 5. PVT1 functions as a competing endogenous RNA to sequester miR-27b-3p within PCa cells. (A and B) PVT1 subcellular localization within LNCap and PC3 cells was examined using RNA-fluorescence *in situ* hybridization and RT-qPCR analyses of nuclear and cytoplasmic RNA fractions. (C) An overlap between putative miRNA targets of PVT1 was identified by the LncBase (ver. 2) and miRanda databases and those miRNAs that were downregulated in PCa tissues compared with normal prostate tissue; Down DEMs, downregulated differential expressed miRNAs. (D and E) RT-qPCR was conducted to assess miRNA expression levels in samples following pull-down assay using biotinylated PVT1 and NC probes. (F) Dual-luciferase activity assay was conducted following the co-transfection of PCa cells using miR-NC/miR-27b-3p mimic or PVT1-WT/PVT1-MT. (G and H) RT-qPCR was employed to detect miR-27b-3p expression level in PCa cells following PVT1 overexpression vector, empty vector, PVT1-sh, or NC-sh transfection. *P<0.05, **P<0.01 and ***P<0.001. PVT1, plasmacytoma variant translocation 1; PCa, prostate cancer; RT-qPCR, reverse transcription-quantitative polymerase chain reaction.

subcellular localization RT-qPCR assays (Fig. 5A and B), which is consistent with the ability of PVT1 to primarily influence the characteristics of PCa cells within the cytoplasm. Potential miRNA binding partners for PVT1 were

identified using miRanda and the LncBase Predicted (ver. 2) online databases. Of the putative interacting miRNAs, three were significantly downregulated in PCa samples in TCGA database, and were thus considered as potential binding targets for PVT1 in PCa (Fig. 5C). The present study also observed the significant downregulation of miR-27b-3p, miR-152-3p and miR-23b-3p expression in PCa tumors (Fig. S1A). According to the results of Pearson's' correlation analysis, the associations between PVT1 and each of these three miRNAs in TCGA PCa dataset were all consistent with a potential ceRNA mechanism of action (Fig. S1B). Furthermore, RNA pull-down assay verified that PVT1 could interact with miR-27b-3p in both PCa cell lines tested (Fig. 5D and E). A putative miR-27b-3p binding site was identified within PVT1, and dual-luciferase reporter assay demonstrated that miR-27b-3p overexpression was sufficient to suppress WT-PVT1 reporter activity (Fig. 5F). In RT-qPCR analysis, the miR-27b-3p expression level was significantly suppressed in both LNCap and PC3 cells following PVT1 overexpression, whereas an opposite effect was observed following PVT1 knockdown (Fig. 5G and H). Notably, miR-27b-3p did not affect c-myc expression at both the mRNA and protein level (Fig. S1C). The obtained outcomes thus support the ability of PVT1 for a direct interaction, thereby sequestering miR-27b-3p within PCa cells.

PVT1 controls the expression level of BLM by functioning as a ceRNA for miR-27b-3p. Using the miRDB platform, four putative miR-27b-3p target genes were identified, including ZNF124, SFXN4, EDRF1 and BLM (Fig. 6A). Of these, BLM was found to be inversely associated with the miR-27b-3p expression level in PCa tissues (Fig. 6B). When the BLM expression level was assessed in PCa samples from the Oncomine database (33,38,42,45,46), this gene was upregulated in PCa tumors (Fig. S1D). Western blot analysis and RT-qPCR similarly confirmed the upregulation of BLM in PCa cell lines (Fig. S2A). A higher BLM expression level was associated with worse Gleason scores and worse treatment outcomes (Fig. S1E). Moreover, a higher BLM expression level was associated with more undesirable disease-free survival outcomes in PCa cases (Fig. 6C). Following the overexpression of miR-27b-3p (Fig. S2B), BLM mRNA and protein levels in PCa cells were elevated (Fig. 6D). Moreover, following the overexpression of BLM (Fig. S2C), it was found that BLM promoted PVT1 expression (Fig. S2D). A putative binding site of miR-27b-3p was identified within the BLM 3'-UTR, and the dual-luciferase reporter assay demonstrated the ability of miR-27b-3p to suppress BLM 3'-UTR-WT reporter plasmid activity in PCa cells (Fig. 6E). RIP assay revealed that miR-27b-3p co-precipitated with BLM, confirming the binding association between these two RNAs (Fig. 6F). Moreover, the miR-27b-3p expression level was significantly inhibited following PVT1 overexpression in LNCap and PC3 cells, whereas the same result was not observed in the PVT1-MUT vector group. The BLM expression level was markedly upregulated following PVT1 overexpression, rather than in the PVT1-MUT vector group. These results thus support a role for PVT1 as a regulator of BLM expression owing to its ability to sequester miR-27b-3p.

PVT1 directly stabilizes and interacts with BLM. To determine whether PVT1 can alter the stability of the BLM protein, CHX was used to treat the LNCap and PC3 cells, in order to block translational activity, and BLM degradation was then monitored over time. The BLM degradation rates significantly decreased in the cells following PVT1 knockdown compared with the control cells, while the BLM expression level in shPVT1-transfected PCa cells increased, following MG132-mediated proteasome inhibition (Fig. 7A and B). According to the results of the immunoprecipitation assay, PVT1 also retained its ubiquitination level (Fig. 7C and D). RNA pull-down assay was additionally conducted, following the incubation of LNCap and PC3 cell lysates with antisense PVT1 or biotin-labeled PVT1, and revealed the ability of BLM and PVT1 to directly interact within PCa cells (Fig. 7E). In addition, a RIP assay was performed using anti-BLM, which similarly confirmed the ability of BLM and PVT1 to interact together (Fig. 7F). These data thus provide evidence for direct interactions between PVT1 and BLM, in which lncRNA may partly function to reduce BLM ubiquitination, thereby improving its stability.

PVT1 modulates the miR-27b-3p/BLM axis to promote PCa progression. To examine the interaction between BLM and miR-27b-3p in the context of the PVT1-mediated regulation of PCa cell malignancy, a series of rescue experiments were performed. Initially, RT-qPCR and western blot analysis were used to confirm successful BLM upregulation in cells transfected with a BLM overexpression vector (BLM-OE) (Fig. 8A). PC3 cells were then transfected with either BLM-OE or empty vector control together with PVT1-sh2, and the malignant activities of these cells were assessed. While PVT1 knockdown reduced the colony formation and proliferative activity of these cells (Fig. 8B and C), BLM overexpression partially reversed these changes. Similarly, PVT1 knockdown impaired the PC3 migratory and invasive capabilities, whereas BLM overexpression reversed these changes (Fig. 8D and E). Western blot analysis was additionally performed to evaluate the expression levels of cell cycle- and apoptosis-related proteins in these cells, and revealed significant reductions in the expression levels of cyclin D1, CDK4/6 and Bcl-2, following PVT1 knockdown that were reversed by BLM overexpression (Fig. 8F). BLM additionally reversed the PVT1 knockdown-mediated enhancement in the E-cadherin expression level, and also reduced the expression levels of Slug, Vimentin and N-cadherin (Fig. 8G). These data thus indicated that PVT1 promoted PCa progression in part by inducing the downregulation of BLM expression.

PVT1 promotes PCa progression in vivo via the miR-27b-3p/BLM pathway. Finally, the performance of PVT1 as a regulator of PCa progression *in vivo* was assessed by subcutaneously implanting nude mice with PC3 cells that had been transfected with empty vector (Vector) or BLM-OE together with PVT1-sh2. Tumor volume and weight were then monitored over time, which revealed significantly a slower tumor growth and lower weight values following PVT1 downregulation, while this outcome was reversed by BLM overexpression (Fig. 9A-C). The expression levels of BLM and PVT1 in tumor tissues from these mice were detected using

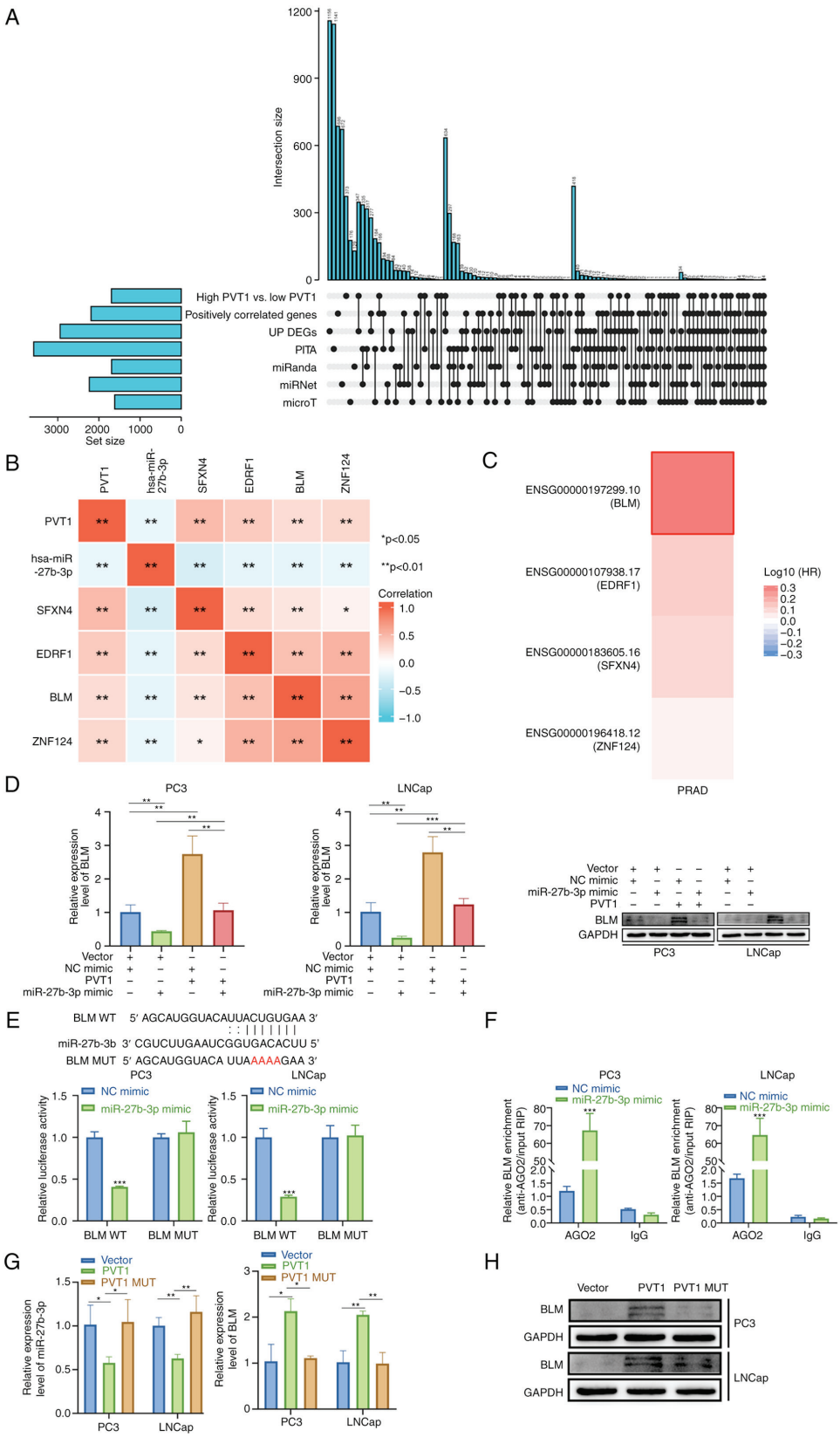

Figure 6. BLM is a miR-27b-3p target gene. (A) The miRanda, miRwalk, miRDB, RNA22, and TargetScan databases were employed to estimate possible miR-27b-3p target genes. (B) Associations between the expression levels of PVT1 and miR-27b-3p, and the identified target genes. (C) Analysis of disease-free survival as a function of the expression levels of BLM, EDRF1, SFXN4 and ZNF124. (D) reverse transcription-quantitative polymerase chain reaction and western blot analysis were utilized to assess the BLM expression level in LNCap and PC3 cells following PVT1 overexpression vector and miR-27b-3p mimic or NC mimic co-transfection. (E) Luciferase activity in PCa cells was quantified following miR-NC/miR-27b-3p mimic or BLM-WT/BLM-MT co-transfection. (F) Interactions between miR-27b-3p and BLM were assessed using RIP assay. (G) The expression levels of BLM and miR-27b-3p in PCa cells following PVT1 overexpression vector or PVT1-MUT treatment. (H) BLM expression level in PCa cells following PVT1 overexpression vector or PVT1-MUT treatment as assessed using western blot analysis. Data were from triplicate measurement and are presented as the mean ± SD. *P<0.05, **P<0.01 and ***P<0.001. BLM, bloom syndrome protein; EDRF1, erythroid differentiation regulatory factor 1; SFXN4, sideroflexin 4; ZNF124, zinc finger protein 124; PVT1, plasmacytoma variant translocation 1; PCa, prostate cancer.

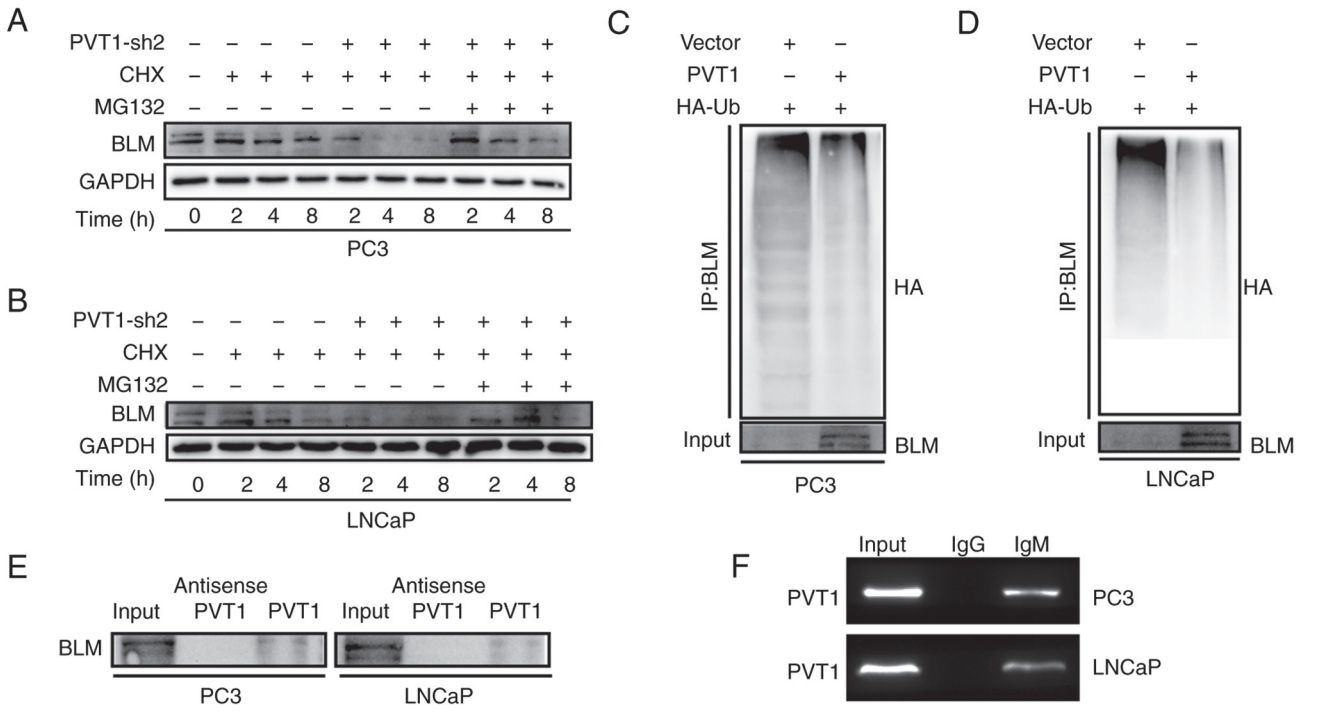

Figure 7. PVT1 interacts with BLM. (A and B) CHX was used to treat the LNCap or PC3 cells that had been treated with PVT1-sh2 and/or MG132 for 2, 4 or 8 h, in which the cells were lysed, the BLM expression level was analyzed, and GAPDH was considered for the normalization of the expression levels. (C and D) IP assay revealed that PVT1 reduced BLM ubiquitination in LNCap and PC3 cells. (E) Lysates prepared from PCa cells were incubated with antisense PVT1 or biotin-labeled PVT1 and pulled down, and the BLM expression level was detected using western blot analysis. (F) Anti-BLM was used to conduct RIP assay in the indicated PCa cell lines. PVT1, plasmacytoma variant translocation 1; PCa, prostate cancer; BLM, bloom syndrome protein; CHX, cycloheximide.

RT-qPCR, and it was found that the BLM expression level was downregulated following PVT1 knockdown, whereas BLM overexpression reversed this change in the tumor cells (Fig. 9D). The immunohistochemical staining of these tumors yielded consistent results, and additionally indicated that there were fewer PCNA-positive tumor cells in tumors, in which PVT1 was knocked down, while this outcome was reversed by the overexpression of BLM (Fig. 9E). PVT1 knockdown additionally increased the cleaved caspase-9 expression level and reduced the N-cadherin expression level within these tumors, while BLM overexpression exerted the opposite effect (Fig. 9E). These findings indicated that PVT1 promoted PCa progression via the miR-27b-3p/BLM axis.

Discussion

As an important prognostic factor in the context of tumor development and patient survival for various types of cancer, PVT1 can regulate a range of biological activities, including motility, invasion, proliferation and cell death (47,48). In patients with PCa, the prognostic value of PVT1 has previously been demonstrated (49-51), which is in line with the results of the present study, indicating the upregulation of PVT1 in PCa tumor samples and the association between the expression level of this lncRNA, clinical staging and patient survival outcomes. Other research groups have similarly reported that PVT1 upregulation is predictive of a decreased patient overall survival, and it is positively associated with lymph node metastasis, distant metastasis, TNM staging and tumor size (24,51,52). Overall, the obtained findings demonstrated that PVT1 may be a prognostic biomarker for PCa, although further research regarding the mechanistic basis for its dysregulation is warranted.

The m^6A modification can regulate the expression levels of several tumor-associated genes (13,53), and the dysregulation of this process is strongly associated with tumor progression (54). A complex of methyltransferase comprising WTAP, METTL3 and other proteins catalyzes the m^6A modification of lncRNAs and other targets within the nucleus (55). Different patterns of m^6A distributions have been observed for mRNAs and lncRNAs, suggesting that distinct mechanisms may govern these two modification processes, although additional analysis are required to fully clarify this hypothesis (56,57). The present study highlighted a novel PVT1-related regulatory pathway in PCa cells. Through RIP and RNA pull-down experiments, it was found that PVT1 was subjected to METTL3-mediated m^6A modification, with METTL3 ultimately suppressed PVT1 degradation, resulting in a net increase in the expression level of this lncRNA. Consequently, it was revealed that METTL3 knockdown suppressed PVT1 m^6A modification, leading to the impairment of its reader binding protein and a consequent increase in PVT1 turnover owing to its co-localization with decay factors (58). Additional research, however, is required to verify this hypothetical model.

Recent research has presented evidence for the capability of lncRNAs to sequester specific miRNAs in a sponge-like manner, thereby functioning as ceRNAs and altering the functionality of these miRNAs (59). PVT1, for instance, has been previously reported to bind to tumor suppressor miRNAs, thereby upregulating the nucleolar protein 2 (NOP2) expression level, as well as promoting PCa metastasis (60).

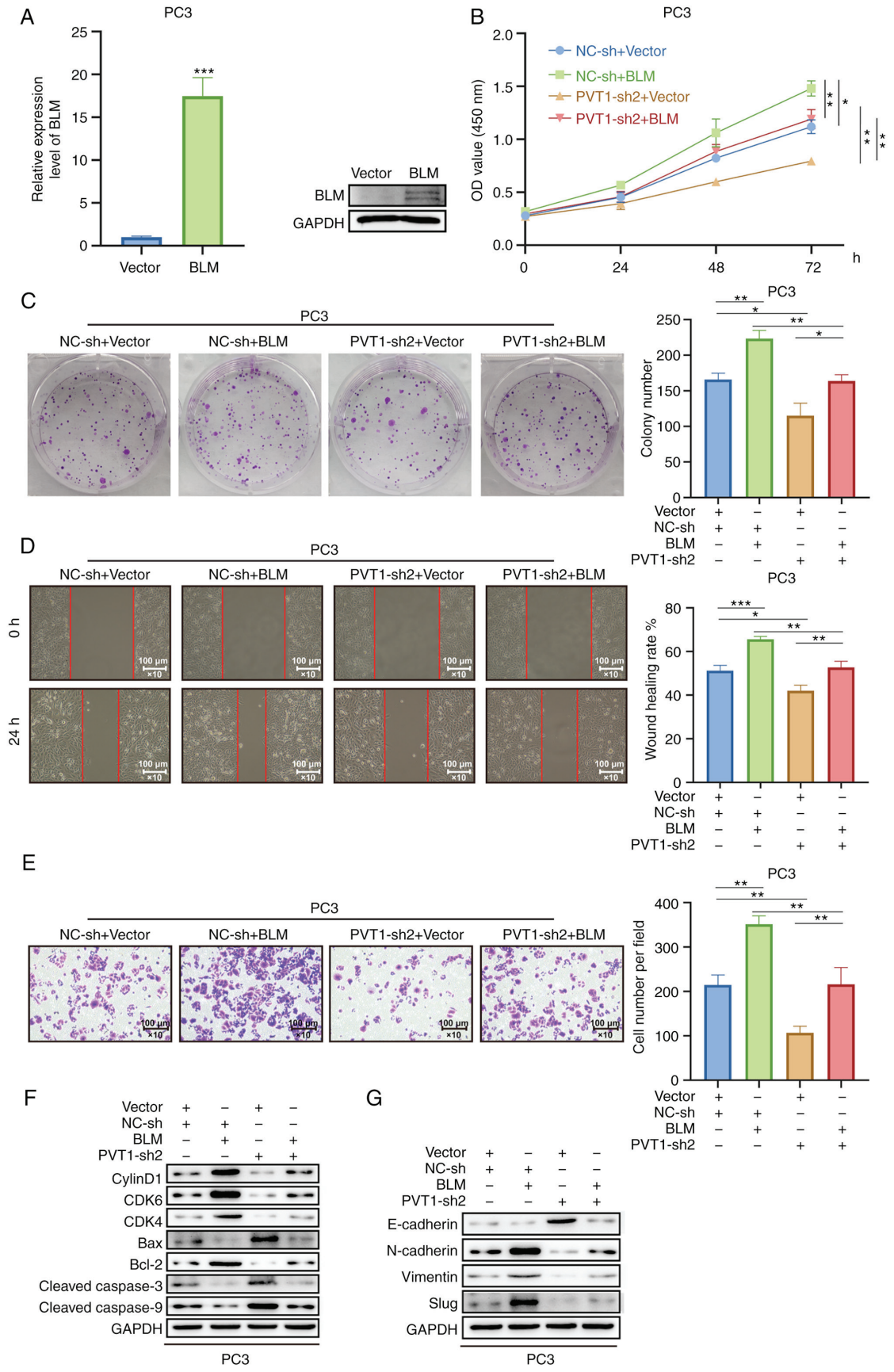

Figure 8. BLM overexpression reverses the effects of PVT1 upregulation on tje proliferative, migratory and invasive abilities of PCa cells. (A) BLM upregulation was detected using reverse transcription-quantitative polymerase chain reaction and western blot analysis in PC3 cells following BLM vector introduction. (B-G) PVT1-sh2 and BLM overexpression or control vectors were co-transfected into PC3 cells, of which the proliferative, colony formation, migratory and invasive abilities of PCa cells were assessed using (B) CCK-8, (C) colony formation, (D) wound healing, and (E) Transwell assays, respectively. (F) Cell cycle- and apoptosis-related protein expression levels in PC3 cells were measured. (G) The expression levels of E-cadherin, N-cadherin, vimentin and Slug in PC3 cells were measured using western blot analysis. *P<0.05, **P<0.01 and ***P<0.001. BLM, bloom syndrome protein; PVT1, plasmacytoma variant translocation 1; PCa, prostate cancer.

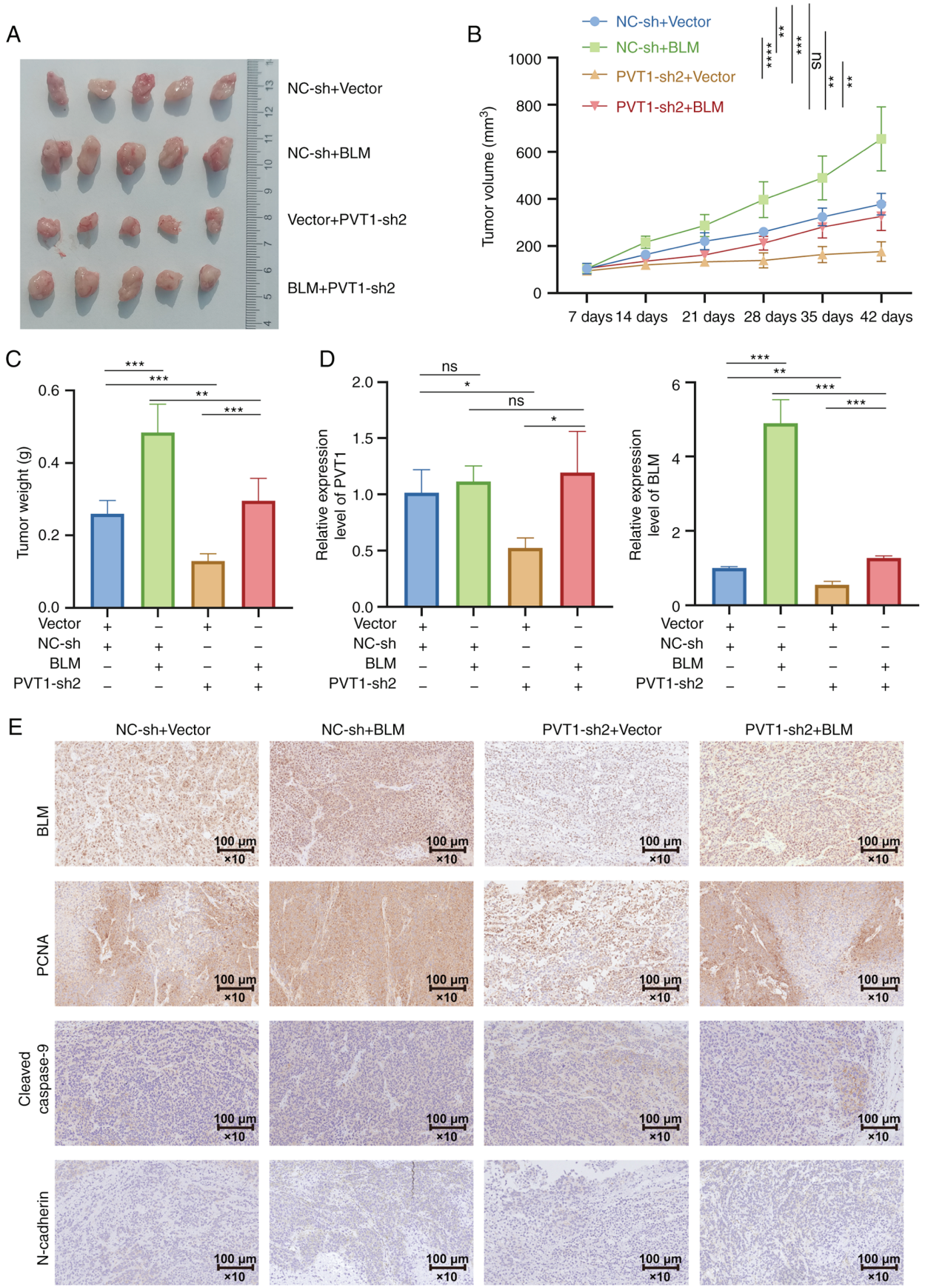

Figure 9. Knockdown of PVT1 suppresses PCa tumor growth *in vivo* through mechanisms dependent on the miR-27b-3p/BLM axis. (A) Tumors observed at 6 weeks post-implantation in BALB/c nude mice in the indicated groups at the experimental endpoint. (B) At 7 days following implantation, tumor volume was monitored once per week. (C) Tumors were weighed at the end of the experiment. (D) The expression levels of PVT1 and BLM were monitored using reverse transcription-quantitative polymerase chain reaction in isolated tumors. (E) Immunohistochemical staining was employed to detect the expression levels of N-cadherin, cleaved caspase-9, PCNA and BLM in xenograft tumors (magnification, x200; scale bars, 100 μm). *P<0.05, **P<0.01 and ***P<0.001. ns, not significant; PVT1, plasmacytoma variant translocation 1; PCa, prostate cancer; BLM, bloom syndrome protein; PCNA, proliferating cell nuclear antigen.

Furthermore, PVT1 has been demonstrated to enhance PCa cell growth in a miR-146a methylation-dependent manner (61), in addition to promoting PCa progression and EMT induction via the suppression of the miR-187-mediated inhibition of Twist1 expression (62). Furthermore, PVT1 acts as a sponge for miRNA-186-5p and positively regulates Twist1 to promote prostate cancer progression (62). PVT1 can regulate ferroptosis through miR-214-mediated TFR1 and p53 (63). PVT1 can promote gallbladder cancer progression by regulating the miR-143/HK2 axis (64). To clarify the mechanisms whereby PCa influences PCa cell malignancy, the present study conducted bioinformatics analyses, leading to the identification of miR-27b-3p as an additional PVT1 target miRNA that has previously been illustrated to play a tumor suppressive role in lung cancer and esophageal squamous cell carcinoma (65,66). Although the interaction of PVT1 and miR-27b-3p has been previously reported (67,68), this finding was only demonstrated in non-tumor cells. In the present study, RT-qPCR divulged a negative regulatory association between PVT1 and miR-27b-3p, and dual-luciferase reporter, pull-down and RIP assays additionally confirmed the direct targeting association between these two RNAs in PCa cells.

BLM controls essential intracellular processes, including telomerase maintenance, DNA unwinding and DNA repair, in addition to serving as a promising biomarker for PCa (69,70). BLM has been reported to target the MYC proto-oncogene gene that encodes c-MYC, thereby enabling it to function as a tumor suppressor gene (71). In a previous study, the authors found that miR-27b-3p could target BLM (72). However, the finding was only limited to cells and the binding of miR-27b-3p and BLM was only confirmed by dual-luciferase reporter assay. In the present study, by integrating prediction results from databases, the expression level-based correlation of PVT1, miR-27b-3p and BLM in PCa tissues from TCGA database, and the BLM expression level from TCGA and Oncomine databases, BLM was detected as a miR-27b-3p target. Furthermore, this association was confirmed using the dual-luciferase reporter and AGO2 pull-down assays. Whether this regulatory association is linked to the c-myc expression level, however, warrants further investigation.

In conclusion, the findings of the present study demonstrate that the METTL3/PVT1/miR-27b-3p/BLM axis may act as a positive regulator of PCa progression. However, only the METTL3methyltransferase was detected to mediate PVT1 m^{6}A modification, and additional research regarding this regulatory epigenetic relationship is thus warranted.

Acknowledgements

Not applicable.

Funding

The present study was financially supported by the National Natural Science Foundation of China (grant no. 31860242).

Availability of data and materials

The datasets used and/or analyzed during the current study are available from the corresponding author on reasonable request.

Authors' contributions

BC and HX conceived the study and designed the experiments. CL and HL contributed to data collection and confirm the authenticity of all the raw data. GB and YZ performed the data analysis and interpreted the results. BC wrote the manuscript. BC and HX contributed to the critical revision of article. All authors have read and approved the final manuscript.

Ethics approval and consent to participate

The study protocol was approved by the Ethics Committee of Affiliated Hospital of Zunyi Medical University [Compliance Medical Ethics Review (2021) no. 1-037). Written informed consent was obtained from all participants prior to enrollment. The animal study protocol was approved by the Ethics Committee of Affiliated Hospital of Zunyi Medical University (ZMU21-2205-002).

Patient consent for publication

Not applicable.

Competing interests

The authors declare that they have no competing interests.

References

1. Siegel RL, Miller KD and Jemal A: Cancer statistics, 2020. CA Cancer J Clin 70: 7-30, 2020.
2. Kimura T and Egawa S: Epidemiology of prostate cancer in Asian countries. Int J Urol 25: 524-531, 2018.
3. Teo MY, Rathkopf DE and Kantoff P: Treatment of advanced prostate cancer. Annu Rev Med 70: 479-499, 2019.
4. Rebbeck TR: Prostate cancer genetics: Variation by race, ethnicity, and geography. Semin Radiat Oncol 27: 3-10, 2017.
5. Kaiser A, Haskins C, Siddiqui MM, Hussain A and D'Adamo C: The evolving role of diet in prostate cancer risk and progression. Curr Opin Oncol 31: 222-229, 2019.
6. Moammeri A, Abbaspour K, Zafarian A, Jamshidifar E, Motasadizadeh H, Dabbagh Moghaddam F, Salehi Z, Makvandi P and Dinarvand R: pH-Responsive, adorned nanoniosomes for codelivery of cisplatin and epirubicin: Synergistic treatment of breast cancer. ACS Appl Bio Mater 5: 675-690, 2022.
7. Ramezani Farani M, Azarian M, Heydari Sheikh Hossein H, Abdolvahabi Z, Mohammadi Abgarmi Z, Moradi A, Mousavi SM, Ashrafizadeh M, Makvandi P, Saeb MR and Rabiee N: Folic acid-adorned curcumin-loaded iron oxide nanoparticles for cervical cancer. ACS Appl Bio Mater 5: 1305-1318, 2022.
8. Sharifi E, Bigham A, Yousefiasl S, Trovato M, Ghomi M, Esmaeili Y, Samadi P, Zarrabi A, Ashrafizadeh M, Sharifi S, *et al*: Mesoporous bioactive glasses in cancer diagnosis and therapy: Stimuli-responsive, toxicity, immunogenicity, and clinical translation. Adv Sci (Weinh) 9: e2102678, 2022.
9. Snow O, Lallous N, Singh K, Lack N, Rennie P and Cherkasov A: Androgen receptor plasticity and its implications for prostate cancer therapy. Cancer Treat Rev 81: 101871, 2019.
10. Yassin A, AlRumaihi K, Alzubaidi R, Alkadhi S and Al Ansari A: Testosterone, testosterone therapy and prostate cancer. Aging Male 22: 219-227, 2019.
11. Zhang H, Shi X, Huang T, Zhao X, Chen W, Gu N and Zhang R: Dynamic landscape and evolution of m6A methylation in human. Nucleic Acids Res 48: 6251-6264, 2020.
12. Yang Y, Hsu PJ, Chen YS and Yang YG: Dynamic transcriptomic m^{6}A decoration: Writers, erasers, readers and functions in RNA metabolism. Cell Res 28: 616-624, 2018.
13. Sun T, Wu R and Ming L: The role of m6A RNA methylation in cancer. Biomed Pharmacother 112: 108613, 2019.

14. Wang T, Kong S, Tao M and Ju S: The potential role of RNA N6-methyladenosine in Cancer progression. Mol Cancer 19: 88, 2020.
15. Boon RA, Jae N, Holdt L and Dimmeler S: Long Noncoding RNAs: From clinical genetics to therapeutic targets? J Am Coll Cardiol 67: 1214-1226, 2016.
16. Jiang R, Tang J, Chen Y, Deng L, Ji J, Xie Y, Wang K, Jia W, Chu WM and Sun B: The long noncoding RNA lnc-EGFR stimulates T-regulatory cells differentiation thus promoting hepatocellular carcinoma immune evasion. Nat Commun 8: 15129, 2017.
17. Li J, Tian H, Yang J and Gong Z: Long Noncoding RNAs regulate cell growth, proliferation, and apoptosis. DNA Cell Biol 35: 459-470, 2016.
18. Paraskevopoulou MD and Hatzigeorgiou AG: Analyzing MiRNA-LncRNA interactions. Methods Mol Biol 1402: 271-286, 2016.
19. Ashrafizadeh M, Paskeh MDA, Mirzaei S, Gholami MH, Zarrabi A, Hashemi F, Hushmandi K, Hashemi M, Nabavi N, Crea F, *et al*: Targeting autophagy in prostate cancer: Preclinical and clinical evidence for therapeutic response. J Exp Clin Cancer Res 41: 105, 2022.
20. Ashrafizaveh S, Ashrafizadeh M, Zarrabi A, Husmandi K, Zabolian A, Shahinozzaman M, Aref AR, Hamblin MR, Nabavi N, Crea F, *et al*: Long non-coding RNAs in the doxorubicin resistance of cancer cells. Cancer Lett 508: 104-114, 2021.
21. Mirzaei S, Zarrabi A, Hashemi F, Zabolian A, Saleki H, Ranjbar A, Seyed Saleh SH, Bagherian M, Sharifzadeh SO, Hushmandi K, *et al*: Regulation of Nuclear Factor-KappaB (NF-κB) signaling pathway by non-coding RNAs in cancer: Inhibiting or promoting carcinogenesis? Cancer Lett 509: 63-80, 2021.
22. Zhang Y, Tan Y, Wang H, Xu M and Xu L: Long Non-Coding RNA plasmacytoma variant translocation 1 (PVT1) enhances proliferation, migration, and epithelial-mesenchymal transition (EMT) of pituitary adenoma cells by activating β-catenin, c-Myc, and cyclin D1 expression. Med Sci Monit 25: 7652-7659, 2019.
23. Wu H, Tian X and Zhu C: Knockdown of lncRNA PVT1 inhibits prostate cancer progression in vitro and in vivo by the suppression of KIF23 through stimulating miR-15a-5p. Cancer Cell Int 20: 283, 2020.
24. Liu J, Li Y, Zhang Q, Lv C, Wang M, Jiao Y and Wang C: PVT1 expression is a predictor for poor survival of prostate cancer patients. Technol Cancer Res Treat 20: 1533033820971610, 2021.
25. Zhao J, Du P, Cui P, Qin Y, Hu C, Wu J, Zhou Z, Zhang W, Qin L and Huang G: LncRNA PVT1 promotes angiogenesis via activating the STAT3/VEGFA axis in gastric cancer. Oncogene 37: 4094-4109, 2018.
26. Chen S, Zhou L and Wang Y: ALKBH5-mediated m^{6}A demethylation of lncRNA PVT1 plays an oncogenic role in osteosarcoma. Cancer Cell Int 20: 34, 2020.
27. Qi X, Zhang DH, Wu N, Xiao JH, Wang X and Ma W: ceRNA in cancer: Possible functions and clinical implications. J Med Genet 52: 710-718, 2015.
28. Liu K and Xu Q: LncRNA PVT1 regulates gallbladder cancer progression through miR-30d-5p. J Biol Regul Homeost Agents 34: 875-883, 2020.
29. Zhou C, Yi C, Yi Y, Qin W, Yan Y, Dong X, Zhang X, Huang Y, Zhang R, Wei J, *et al*: LncRNA PVT1 promotes gemcitabine resistance of pancreatic cancer via activating Wnt/beta-catenin and autophagy pathway through modulating the miR-619-5p/Pygo2 and miR-619-5p/ATG14 axes. Mol Cancer 19: 118, 2020.
30. Schmittgen TD and Livak KJ: Analyzing real-time PCR data by the comparative C(T) method. Nat Protoc 3: 1101-1108, 2008.
31. Song YX, Sun JX, Zhao JH, Yang YC, Shi JX, Wu ZH, Chen XW, Gao P, Miao ZF and Wang ZN: Non-coding RNAs participate in the regulatory network of CLDN4 via ceRNA mediated miRNA evasion. Nat Commun 8: 289, 2017.
32. Hu Y, Rao SS, Wang ZX, Cao J, Tan YJ, Luo J, Li HM, Zhang WS, Chen CY and Xie H: Exosomes from human umbilical cord blood accelerate cutaneous wound healing through miR-21-3p-mediated promotion of angiogenesis and fibroblast function. Theranostics 8: 169-184, 2018.
33. Arredouani MS, Lu B, Bhasin M, Eljanne M, Yue W, Mosquera JM, Bubley GJ, Li V, Rubin MA, Libermann TA and Sanda MG: Identification of the transcription factor single-minded homologue 2 as a potential biomarker and immunotherapy target in prostate cancer. Clin Cancer Res 15: 5794-5802, 2009.
34. Lapointe J, Li C, Higgins JP, van de Rijn M, Bair E, Montgomery K, Ferrari M, Egevad L, Rayford W, Bergerheim U, *et al*: Gene expression profiling identifies clinically relevant subtypes of prostate cancer. Proc Natl Acad Sci USA 101: 811-816, 2004.
35. LaTulippe E, Satagopan J, Smith A, Scher H, Scardino P, Reuter V and Gerald WL: Comprehensive gene expression analysis of prostate cancer reveals distinct transcriptional programs associated with metastatic disease. Cancer Res 62: 4499-4506, 2002.
36. Luo JH, Yu YP, Cieply K, Lin F, Deflavia P, Dhir R, Finkelstein S, Michalopoulos G and Becich M: Gene expression analysis of prostate cancers. Mol Carcinog 33: 25-35, 2002.
37. Singh D, Febbo PG, Ross K, Jackson DG, Manola J, Ladd C, Tamayo P, Renshaw AA, D'Amico AV, Richie JP, *et al*: Gene expression correlates of clinical prostate cancer behavior. Cancer Cell 1: 203-209, 2002.
38. Taylor BS, Schultz N, Hieronymus H, Gopalan A, Xiao Y, Carver BS, Arora VK, Kaushik P, Cerami E, Reva B, *et al*: Integrative genomic profiling of human prostate cancer. Cancer Cell 18: 11-22, 2010.
39. Tomlins SA, Mehra R, Rhodes DR, Cao X, Wang L, Dhanasekaran SM, Kalyana-Sundaram S, Wei JT, Rubin MA, Pienta KJ, *et al*: Integrative molecular concept modeling of prostate cancer progression. Nat Genet 39: 41-51, 2007.
40. Varambally S, Yu J, Laxman B, Rhodes DR, Mehra R, Tomlins SA, Shah RB, Chandran U, Monzon FA, Becich MJ, *et al*: Integrative genomic and proteomic analysis of prostate cancer reveals signatures of metastatic progression. Cancer Cell 8: 393-406, 2005.
41. Welsh JB, Sapinoso LM, Su AI, Kern SG, Wang-Rodriguez J, Moskaluk CA, Frierson HF Jr and Hampton GM: Analysis of gene expression identifies candidate markers and pharmacological targets in prostate cancer. Cancer Res 61: 5974-5978, 2001.
42. Yu YP, Landsittel D, Jing L, Nelson J, Ren B, Liu L, McDonald C, Thomas R, Dhir R, Finkelstein S, *et al*: Gene expression alterations in prostate cancer predicting tumor aggression and preceding development of malignancy. J Clin Oncol 22: 2790-2799, 2004.
43. Wang R and Liu X: Epigenetic regulation of prostate cancer. Genes Dis 7: 606-613, 2019.
44. Li J, Xie H, Ying Y, Chen H, Yan H, He L, Xu M, Xu X, Liang Z, Liu B, *et al*: YTHDF2 mediates the mRNA degradation of the tumor suppressors to induce AKT phosphorylation in N6-methyladenosine-dependent way in prostate cancer. Mol Cancer 19: 152, 2020.
45. Grasso CS, Wu YM, Robinson DR, Cao X, Dhanasekaran SM, Khan AP, Quist MJ, Jing X, Lonigro RJ, Brenner JC, *et al*: The mutational landscape of lethal castration-resistant prostate cancer. Nature 487: 239-243, 2012.
46. Liu P, Ramachandran S, Ali Seyed M, Scharer CD, Laycock N, Dalton WB, Williams H, Karanam S, Datta MW, Jaye DL and Moreno CS: Sex-determining region Y box 4 is a transforming oncogene in human prostate cancer cells. Cancer Res 66: 4011-4019, 2006.
47. Ding C, Yang Z, Lv Z, DU C, Xiao H, Peng C, Cheng S, Xie H, Zhou L, Wu J and Zheng S: Long non-coding RNA PVT1 is associated with tumor progression and predicts recurrence in hepatocellular carcinoma patients. Oncol Lett 9: 955-963, 2015.
48. Li KK, Lau KM and Ng HK: Signaling pathway and molecular subgroups of medulloblastoma. Int J Clin Exp Pathol 6: 1211-1222, 2013.
49. Lin HY, Callan CY, Fang Z, Tung HY and Park JY: Interactions of PVT1 and CASC11 on prostate cancer risk in african americans. Cancer Epidemiol Biomarkers Prev 28: 1067-1075, 2019.
50. Videira A, Beckedorff FC, daSilva LF and Verjovski-Almeida S: PVT1 signals an androgen-dependent transcriptional repression program in prostate cancer cells and a set of the repressed genes predicts high-risk tumors. Cell Commun Signal 19: 5, 2021.
51. Yang J, Li C, Mudd A and Gu X: LncRNA PVT1 predicts prognosis and regulates tumor growth in prostate cancer. Biosci Biotechnol Biochem 81: 2301-2306, 2017.
52. Yan YJ, Zhang L, Zhou JJ, Chen ZJ, Liao YX, Zeng JM and Shen H: Comprehensive characterization of common and cancer-specific differently expressed lncRNAs in urologic cancers. Comput Math Methods Med 2021: 5515218, 2021.
53. Lyko F and Brown R: DNA methyltransferase inhibitors and the development of epigenetic cancer therapies. J Natl Cancer Inst 97: 1498-1506, 2005.
54. Tuncel G and Kalkan R: Importance of m N^6-methyladenosine (m^{6}A) RNA modification in cancer. Med Oncol 36: 36, 2019.

55. Sun HL, Zhu AC, Gao Y, Terajima H, Fei Q, Liu S, Zhang L, Zhang Z, Harada BT, He YY, *et al*: Stabilization of ERK-Phosphorylated METTL3 by USP5 Increases m^{6}A Methylation. Mol Cell 80: 633-647 e7, 2020.
56. Liu N, Parisien M, Dai Q, Zheng G, He C and Pan T: Probing N6-methyladenosine RNA modification status at single nucleotide resolution in mRNA and long noncoding RNA. RNA 19: 1848-1856, 2013.
57. Amort T, Rieder D, Wille A, Khokhlova-Cubberley D, Riml C, Trixl L, Jia XY, Micura R and Lusser A: Distinct 5-methylcytosine profiles in poly(A) RNA from mouse embryonic stem cells and brain. Genome Biol 18: 1, 2017.
58. Wang X, Lu Z, Gomez A, Hon GC, Yue Y, Han D, Fu Y, Parisien M, Dai Q, Jia G, *et al*: N6-methyladenosine-dependent regulation of messenger RNA stability. Nature 505: 117-120, 2014.
59. Chan JJ and Tay Y: Noncoding RNA:RNA regulatory networks in cancer. Int J Mol Sci 19: 1310, 2018.
60. Sun F, Wu K, Yao Z, Mu X, Zheng Z, Sun M, Wang Y, Liu Z and Zhu Y: Long Noncoding RNA PVT1 promotes prostate cancer metastasis by increasing NOP2 expression via targeting tumor suppressor MicroRNAs. Onco Targets Ther 13: 6755-6765, 2020.
61. Liu HT, Fang L, Cheng YX and Sun Q: LncRNA PVT1 regulates prostate cancer cell growth by inducing the methylation of miR-146a. Cancer Med 5: 3512-3519, 2016.
62. Chang Z, Cui J and Song Y: Long noncoding RNA PVT1 promotes EMT via mediating microRNA-186 targeting of Twist1 in prostate cancer. Gene 654: 36-42, 2018.
63. Lu J, Xu F and Lu H: LncRNA PVT1 regulates ferroptosis through miR-214-mediated TFR1 and p53. Life Sci 260: 118305, 2020.
64. Chen J, Yu Y, Li H, Hu Q, Chen X, He Y, Xue C, Ren F, Ren Z, Li J, *et al*: Long non-coding RNA PVT1 promotes tumor progression by regulating the miR-143/HK2 axis in gallbladder cancer. Mol Cancer 18: 33, 2019.
65. Han M, Li N, Li F, Wang H and Ma L: MiR-27b-3p exerts tumor suppressor effects in esophageal squamous cell carcinoma by targeting Nrf2. Hum Cell 33: 641-651, 2020.
66. Sun Y, Xu T, Cao YW and Ding XQ: Antitumor effect of miR-27b-3p on lung cancer cells via targeting Fzd7. Eur Rev Med Pharmacol Sci 21: 4113-4123, 2017.
67. Li S, Zhao X, Cheng S, Li J, Bai X and Meng X: Downregulating long non-coding RNA PVT1 expression inhibited the viability, migration and phenotypic switch of PDGF-BB-treated human aortic smooth muscle cells via targeting miR-27b-3p. Hum Cell 34: 335-348, 2021.
68. Lu X, Yu Y, Yin F, Yang C, Li B, Lin J and Yu H: Knockdown of PVT1 inhibits IL-1β-induced injury in chondrocytes by regulating miR-27b-3p/TRAF3 axis. Int Immunopharmacol 79: 106052, 2020.
69. Ledet EM, Antonarakis ES, Isaacs WB, Lotan TL, Pritchard C and Sartor AO: Germline BLM mutations and metastatic prostate cancer. Prostate 80: 235-237, 2020.
70. Ruan Y, Xu H, Ji X and Zhao J: BLM interaction with EZH2 regulates MDM2 expression and is a poor prognostic biomarker for prostate cancer. Am J Cancer Res 11: 1347-1368, 2021.
71. Deng L, Meng T, Chen L, Wei W and Wang P: The role of ubiquitination in tumorigenesis and targeted drug discovery. Signal Transduct Target Ther 5: 11, 2020.
72. Chen Y, Zhao J, Duan Z, Gong T, Chen W, Wang S and Xu H: miR27b3p and miR607 cooperatively regulate BLM gene expression by directly targeting the 3'UTR in PC3 cells. Mol Med Rep 19: 4819-4831, 2019.